Influencing factors to the capillary water uptake of (un)cracked cementitious materials

Laurena De Brabandere[1*], *Tim* Van Mullem[1], *Natalia* Alderete[1], *Dries* Baeyens[1], and *Nele* De Belie[1]

[1]Magnel-Vandepitte Laboratory, Department of Structural Engineering and Building Materials, Faculty of Engineering and Architecture, Ghent University, Technologiepark Zwijnaarde 60, Campus Ardoyen, B-9052 Gent, Belgium

Abstract. Capillary water absorption tests are widely used in uncracked cementitious materials to assess the quality and durability. Due to the easy execution of the test, it is also frequently used to assess the self-healing efficiency of self-healing concrete and mortar. It is established that the presence of a crack significantly increases the water uptake by a specimen. However, it is not known how the crack width, healing agents and mix composition influence the capillary water absorption. In this research, for cylindrical mortar specimens with four different crack widths, both a capillary water absorption test and water permeability were test were executed in order to investigate the relation between these two test methods. After the first round of testing, cracked specimens were healed manually with polyurethane and methyl methacrylate and the capillary absorption test was performed again to investigate the sensitivity of the test method to different degrees of crack healing. Furthermore, prismatic specimens were cast to investigate the influence of crack creation and geometry. It was found that the crack width does not have an influence on the capillary absorption rate. However, the crack width has a significant influence on the water flow through the crack. As expected, manual healing with polyurethane is better in comparison to the sealing of the crack mouth with methyl methacrylate.

1 Introduction

Concrete is one of the most used construction materials worldwide. However, due to its low tensile strength, it is prone to cracking. These cracks can occur due to mechanical loading, harsh environmental conditions or shrinkage. Cracks are a fast entry point for aggressive substances such as chlorides or sulphates which can cause reinforcement corrosion or concrete deterioration [1]. More durable 'self-healing' concrete is widely investigated as a replacement for more traditional concrete because of its ability to heal the formed cracks. Different approaches to heal the cracks have been studied such as the addition of bacteria, superabsorbent polymers, capsules or vascular networks [2-5]. Capillary absorption, or imbibition, is widely tested to characterise the transport properties and pore connectivity of mortar and concrete [6]. This test is also frequently used to asses the sealing efficiency of self-healing concrete. It is already well established that the presence of a crack significantly increases the water absorption. For instance in the research of Van Belleghem et al. the capillary water absorption in (un)cracked mortar was studied using X-ray radiography and finite element analysis [1], and water ingress through standardised cracks was visualised. However, currently there is still a lack of knowledge on how the crack width and the presence of healing agents affect the water uptake. Therefore, in this research the capillary absorption of mortar and concrete with the addition of superabsorbent polymers and different crack widths and crack geometry was investigated using the gravimetrical method. Furthermore, a water permeability test was conducted and the relation between the results of the capillary absorption test and the water permeability test was investigated.

2 Materials and methods

2.1 Specimen preparation

Four different mix designs were made, three mortar mixes and one concrete mix. The mix composition is given in Table 1. MasterGlenium 27 con 20 % (BASF, Germany) was used as superplasticizer. Superabsorbent polymers Floset 27 CC from SNF Floerger (France) were added to the SAP mix. Regarding the SAP mix, the dry SAPs were added to the mix and no additional water was added to compensate for the absorption of water by the SAPs during mixing. The water uptake of the SAPs was estimated at 23 g water / g SAP. Therefore, the effective w/c ratio will be lower in comparison to the REF mix.

With the REF, SAP and DRY mix, cylinders (height 200 mm, diameter 100 mm) were cast. With the REF and concrete mix, prisms of 60x60x220 mm^3 with two

* Corresponding author: laurena.debrabandere@ugent.be

© The Authors, published by EDP Sciences. This is an open access article distributed under the terms of the Creative Commons Attribution License 4.0 (http://creativecommons.org/licenses/by/4.0/).

reinforcement bars (Ø 3 mm) at 12 mm from the bottom side were cast.

For the mortar, prisms of 40x40x160 mm^3 were cast to determine the compressive strength after 7, 28 and 56 days. To test the compressive strength of concrete, cubes (side 100 mm) were cast. The specimens were demoulded after 24 to 48 hours after casting and stored in a curing room (20 °C, >95 % RH) until the age of 28 days was reached.

Table 1. Mix compositions in kg/m^3 and total and effective w/c ratio.

	REF	SAP	DRY	Concrete
CEM I 52.5 N	502	500	497	339
Water	252	250	182	186
Sand (0-2)	1508	1500	1678	745
Gravel (2-8)	-	-	-	1016
SAPs	-	3.5	-	-
Superplasticizer	-	7.5	7.5	2.4
Limestone filler	-	-	-	58
W/C_{tot}	0.5	0.5	0.36	0.55
W/C_{eff}	0.5	0.34	0.36	0.55

2.1.1 Cylindrical specimens

After 25 days of curing, the cylinders were cut into samples with a height of 50 mm. At 28 days the circumference of the samples was covered with aluminium tape and samples were cracked using the Brazilian splitting test. The two halves were put back together using hose clamps with silicon sheets between the two halves. The nominal thickness of the sheets was 100, 200, 300 and 400 µm. 6 samples per nominal crack width were made. After cracking and reassembling the specimens, the crack widths were measured using an optical microscope (Leica DMC 2900). Three pictures were taken at each side of the sample. Subsequently, the crack width was measured five times on each picture. The mean crack width of a sample was determined from the 30 measurements.

2.1.2 Prismatic specimens

After 24 days of curing, the prisms were cracked in a three-point-bending setup with a span of 200 mm. The crack creation was controlled with a linear variable differential transformer (LVDT) positioned at the bottom of the specimens. After cracking, the crack widths were measured using an optical microscope (Leica DMC 2900). Four pictures of the crack were taken. The crack was measured five times on each picture which resulted in a mean value of 20 crack width measurements per sample. Table 2 gives an overview of the target crack width, the LVDT reading prior to unloading and the mean measured crack width after unloading.

Table 2. Target crack width, LVDT reading prior to unloading, mean measured crack width after unloading and the standard deviation, and number of specimens.

Target crack width [µm]	Max. LVDT measurement [µm]	Mean measured crack width [µm]	Number of specimens
50	230	71 ± 23	6
100	255	91 ± 16	6
150	280	130 ± 21	6
200	370	188 ± 26	6
250	415	227 ± 38	6
300	510	306 ± 49	5
400	680	401 ± 57	6
500	850	479 ± 72	5

2.2 Porosity characterization

To quantify the porosity of the mortar samples (REF, SAP and DRY), water absorption under vacuum was determined. Cylinders (Ø 100 mm, height 50 mm) were put under vacuum for 2 hours. Subsequently, the vacuum chamber was filled with water until the specimens were fully immersed and air was let into the chamber to lift the vacuum. 24 hours after the start of the vacuum, the saturated specimens were weighed under water (m_w) and in the air (m_a). Then the specimens were placed in an oven at 40 °C and weighed every 24 hours until the mass loss was lower than 0.1 % (m_{d40}). Subsequently, the specimens were also dried in an oven at 105 °C until a constant mass was reached (m_{d105}). The capillary porosity (CP) and open porosity (OP) were calculated as follows:

$$CP\ (\%) = \frac{m_a - m_{d40}}{m_s - m_w} * 100 \quad (1)$$

$$OP\ (\%) = \frac{m_a - m_{d105}}{m_s - m_w} * 100 \quad (2)$$

2.3 Capillary absorption

The preconditioning and the capillary absorption test was the same for cylinders and prisms. First, the samples were laterally waterproofed using an epoxy coating. The specimens were put under immersion for approximately 72 h. Subsequently, they were dried in an oven at 40 °C until the mass loss was lower than 0.5 m% in a 24 h period. After drying, the specimens were wrapped in plastic foil for at least 24 h to obtain a more homogeneous distribution of the moisture inside the samples. Then, the specimens were placed on rails inside a container with a water level 3 mm higher than the bottom of the sample. Periodical measurements were taken on specific intervals: 15 min, 30 min, 1 h, 1.5 h, 2 h, 4 h, 6 h and 24 h and then every 24 h for a duration of 1 week. The capillary absorption rate is calculated as the slope of the fitting line between the water uptake and the square root of time.

2.4 Korean water permeability testing

2.4.1 Cylindrical specimens

The water permeability of cylindrical specimens was tested with a test method based on the work of Shin et al. [7]. The (surface) dry specimen was placed between a plexiglas plate with a hole of 67 mm at the top and two support bars at the bottom of the specimen, parallel with the crack. A rubber ring was placed between the plate and the top of the specimen to ensure a watertight connection. A cylindrical water reservoir with a height of 25 cm was attached on the top of the plate. Subsequently, the specimen was placed in a reservoir as such that the bottom of the specimen was just in contact with water. Then, the upper reservoir was filled with water and a constant overflow of the reservoir was ensured by a water supply of an external reservoir to obtain a constant water pressure. The water flow through the crack flowed directly into a container on an electronic measuring scale.

2.4.2 Prismatic specimens

The water permeability of the mortar prismatic specimens was tested using Karsten tubes. As with the cylindrical specimens, the test was performed after the capillary absorption was terminated and the specimens were air dried. The tubes were attached to the sample using double sided vinyl tape. To start the test, the tube was filled with water (volume: 4 ml). The decrease of water in the tube was measured with the following interval: every minute during the first 10 minutes, then every 2.5 minutes during 10 minutes and finally after 25 and 30 minutes from the beginning of the test. The water flow in g/min through the crack was calculated as the slope between mass and time.

2.5 Manual crack healing

After testing capillary absorption and water permeability, part of the cylindrical samples were manually healed using methyl methacrylate (MMA) or polyurethane (PU) and the capillary absorption test was repeated. Due to a difference in viscosity, the healing with MMA was only effective at the surface of the crack, while with PU the crack was filled over the entire height of the sample using a syringe. The specimens were healed for 25 %, 50 % or 75 % of the crack length (Figure 1). For every healing method, there was a series of 3 samples.

Fig. 1. Representation of the manual healing with MMA or PU of cylindrical specimens for 25 %, 50 % or 75 % of the crack length.

After the second capillary absorption test, the cylindrical specimens were split open and the crack healing was inspected visually.

Figure 2 gives a schematic overview of the performed tests as described in sections 2.1 until 2.5.

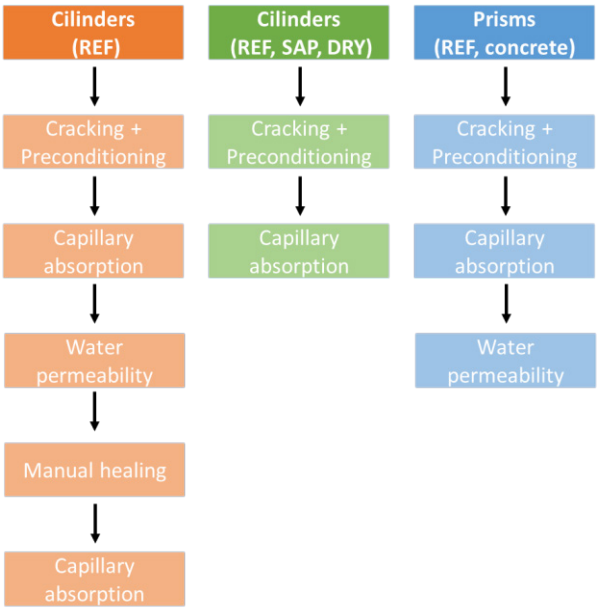

Fig. 2. Schematic overview of the testing program.

3 Results and discussion

3.1 Porosity

The calculated capillary and open porosity of REF, SAP and DRY is given in Figure 3. As expected, CP and OP values of DRY samples are lower in comparison to REF samples due to the lower w/c ratio. The w/c ratio of the REF mix is 0.5, while the SAP and DRY mix have an effective w/c ratio of 0.36. Even though the effective w/c ratio of SAP and DRY mixes are the same, CP and OP of SAP specimens is higher. This is due to the formation of macropores because of the swollen superabsorbent polymers during mixing and hardening.

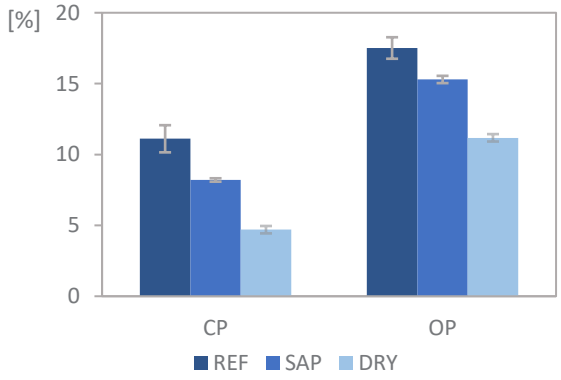

Fig. 3. Capillary porosity (CP) and open porosity (OP) for REF, SAP and DRY.

3.2 Influence of crack width

Figure 4 shows the capillary absorption rate as a function of the crack width for cylindrical specimens of the reference mix. As expected, the absorption rate for uncracked specimens is lower in comparison to cracked specimens. For the cracked specimens the absorption rate does not increase with increasing crack width. However, there is a rather large variation on the obtained results. Van Belleghem et al. [8] found a linear increasing trend ($R^2 = 0.616$) between the crack width and the absorption rate of prismatic specimens was found. However, results shown on Figure 4 do not follow a linear trend. This is possibly due to the difference in crack formation and geometry of the tested samples. In this research, the cylindrical specimens were cracked over the entire height of the specimens, while in the research of Van Belleghem et al. prismatic specimens were not cracked over the entire height of the specimen. Figure 5 shows the water flow as a function of the crack width. The series of 100 µm is not taken into account since there is a significant deviation of the measured crack width from the desired crack width. For the water flow there is a clear trend that shows an increasing water flow with an increasing crack width [9][10].

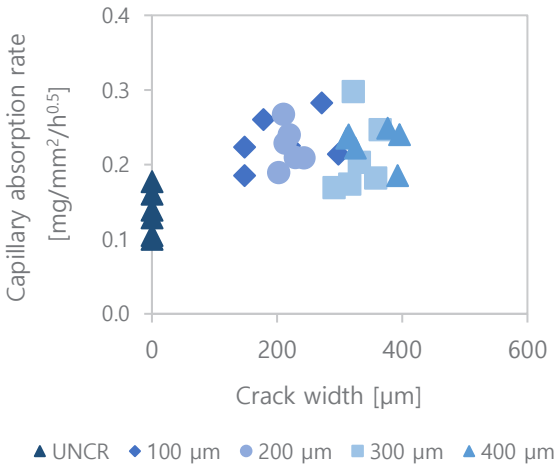

Fig. 4. Capillary absorption rate as a function of the crack width for cylindrical specimens.

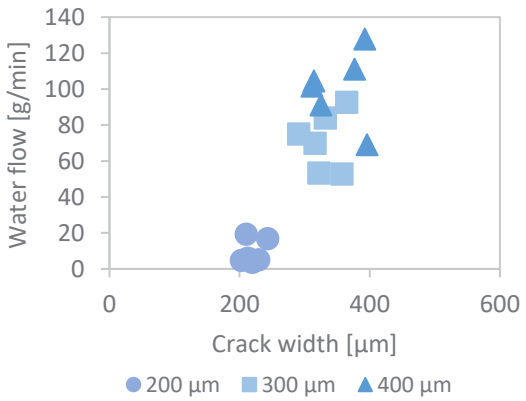

Fig. 5. Water flow as a function of the crack width for cylindrical specimens.

Figure 6 shows the capillary absorption rate as a function of the crack width for prismatic mortar specimens. As with the cylindrical specimens, the absorption rate of the uncracked specimens is much lower in comparison to the cracked specimens. For the cracked specimens, the absorption rate seems to slightly increase linearly with an increasing crack width up. However, a statistical analysis shows that there is no linear trend between both parameters. Figure 7 shows the flow rate as a function of the crack width. There is a minimal increase of water flow with an increasing crack width. The smaller difference between the different crack widths can be attributed to the lower and variable pressure created by the volume of water in the Karsten tube compared to the Korean water permeability test which was executed on the cylindrical specimens.

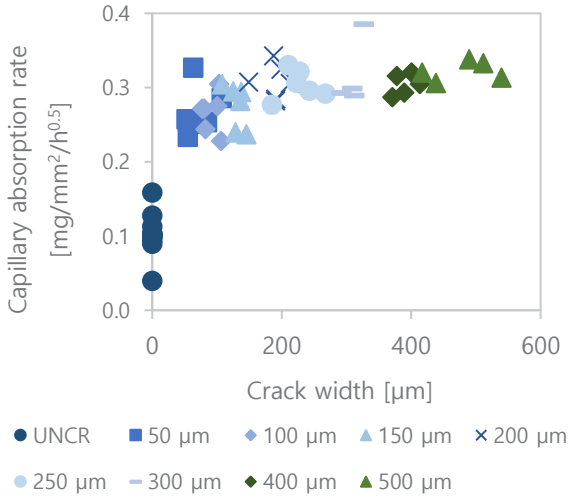

Fig. 6. Capillary absorption rate as a function of the crack width for prismatic specimens.

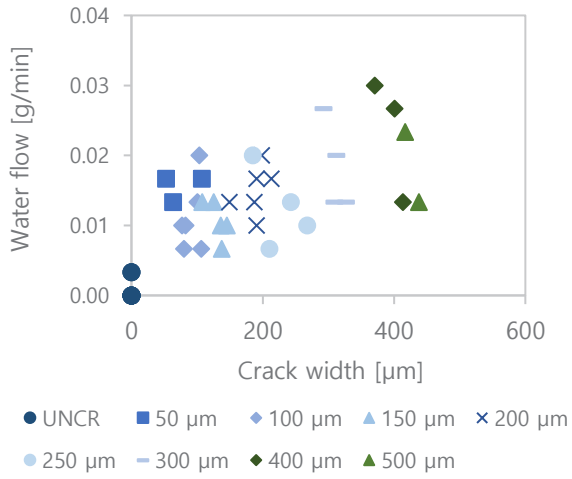

Fig. 7. Water flow as a function of the crack width for prismatic specimens.

3.3 Influence of manual crack healing

Figure 8 shows the reduction of the capillary absorption rate for cylindrical REF specimens with silicon sheets with a nominal thickness of 200 µm before and after

healing with MMA and PU for 25, 50 or 75 %. For healing rates of 50 and 75 %, the reduction and thus the sealing efficiency with MMA is smaller in comparison to PU (level of significance = 5 %, p < 2.3 %). This can be explained by the superficial healing of the crack with MMA. For the healing with PU, manual healing of 50 % of the crack length has the highest reduction rate (65 %); however, a two-sample T-test showed that there is no statistical difference between the healing of 50 % and 75 % (level of significance = 5 %, p = 14.8 %).

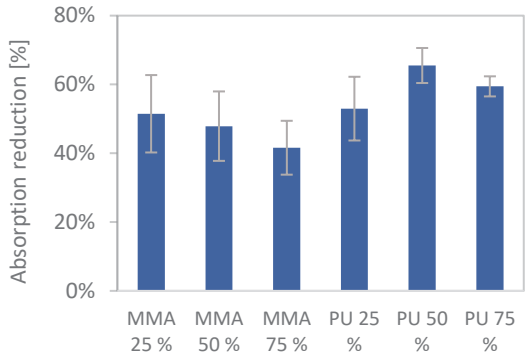

Fig. 8. Reduction of the capillary absorption rate of cylindrical specimens with silicon sheets with a nominal thickness of 200 µm before and after healing with MMA and PU.

The visual inspection of the manual crack healing showed that the MMA did not flow inside the crack, which was expected due to the high viscosity. Figure 9 shows the two halves of a cracked specimen for 25 %, 50 % and 75 % of healing with PU inside the crack. These specimens showed that the desired healing of 25 %, resulted in the presence of PU over 40 % of the crack surface (Figure 9a). For a crack healing of 50 %, this resulted in 65 % of the crack surface being covered with PU (Figure 9b) and 100 % for the desired crack healing of 75 % (Figure 9c).

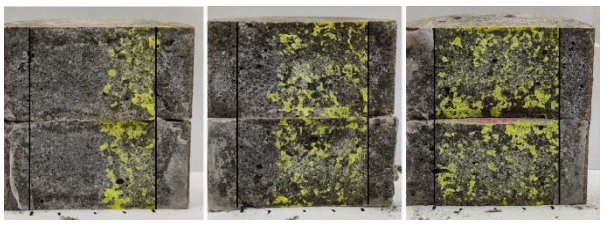

Fig. 9. Visual inspection of the manual crack healing with PU for (a) 25 %; (b) 50 %; (c) 75 % of the crack length.

3.4 Influence of mix composition

Figure 10 shows the capillary absorption rate as a function of the crack width for cylindrical specimens of the mixes REF, SAP and DRY. These cylinders were reassembled with silicon sheets with a nominal thickness of 200 µm. However, it can be seen that the obtained crack widths vary depending on the mix composition. The larger crack widths for the specimens containing the superabsorbent polymers are possibly due to a more rough crack surface. The higher absorption rate for the reference mortar can be explained by the higher effective w/c ratio in comparison to the DRY and SAP mix. However, the results for the water absorption under vacuum showed that the capillary porosity, which is the most important parameter for absorption, of SAP is higher in comparison to DRY. The lower absorption rate of the cracked SAP samples could be explained by the swelling of the superabsorbent polymers during absorption, which blocks the crack and reduces the water absorption through the crack. Similarly, previous research by Snoeck et al. showed that during capillary imbibition tests the water ingress in uncracked samples is reduced in the pores due to swelling of SAP [11].

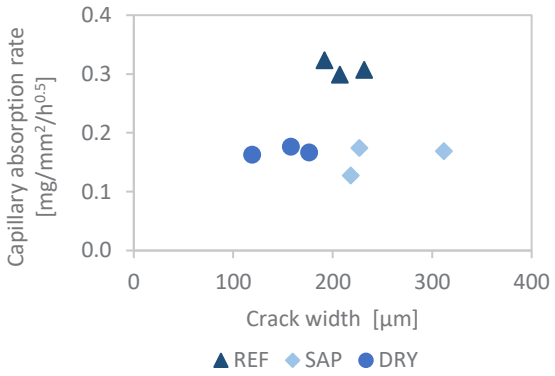

Fig. 10. Capillary absorption rate of prismatic specimens of REF, SAP and DRY as a function the crack width.

The capillary absorption rate of prismatic mortar and concrete specimens is plotted as a function of the measured crack width (Figure 11). The absorption rate of uncracked mortar samples is slightly higher in comparison to concrete, however there is no statistical difference between the mean values (level of significance = 5 %, p = 38,4 %). The capillary absorption rate of mortar is larger in comparison to concrete for cracked samples (level of significance = 5 %, p < 0.4 %). The lower absorption rate of concrete can be explained by the different porosity and restraints due to the presence of coarse aggregates [12].

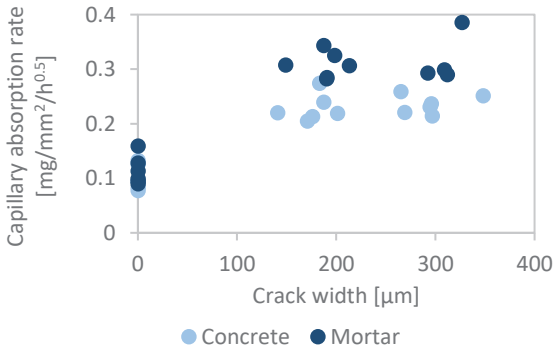

Fig. 11. Capillary absorption rate of prismatic mortar and concrete specimens as a function the crack width.

4 Conclusions

In this research, the following influencing factors on the capillary water absorption were investigated: (1) crack width, (2) manual healing and (3) mix composition (self-healing agents, mortar and concrete). Based on the results obtained during this research, following conclusions could be made:

• The presence of a crack in mortar or concrete significantly increases the water absorption. However, an increased crack width does not lead to an increased absorption for cylindrical specimens. For prismatic specimens there is a small increase in absorption with an increasing crack width. However, a linear trend could not be found statistically. cracks between 50 and 500 µm.

• Unlike the water absorption, water permeability is highly dependent on the crack width.

• Manual healing with polyurethane (PU) filling the crack over the entire height of the sample leads to a higher reduction of the absorption rate in comparison to healing of the crack surface with methyl methacrylate (MMA) for healing rates of 50 and 75 %. However, the efficiency of healing quantified with a capillary absorption test does not increase with an increasing healing percentage.

• Cracked mortar with superabsorbent polymers showed a decreased capillary absorption rate, probably due to the swelling of the superabsorbent polymers at the surface of the crack. The mix containing superabsorbent polymers has a lower effective w/c ratio in comparison to the reference mix. The absorption rate of the SAP mix is comparable to the absorption rate of the DRY mix which has the same effective w/c ratio.

• Cracked samples of mortar have a higher capillary absorption rate in comparison to concrete with a similar crack width due to the difference in porosity and restraint in the system.

This research was supported by a grant (20SCIP-B103706-04) from the Construction Technology Research Program funded by the Ministry of Land, Infrastructure and Transport of the Korean government.

References

1. B. Van Belleghem, R. Montoya, J. Dewanckele, N. Van den Steen, I. De Graeve, J. Deconinck, V. Cnudde, K. Van Tittelboom, N. De Belie, Constr. Build. **110**, 154 (2016)
2. V. Wiktor, H. M. Jonkers, Cem. Concr. Compos. **33**, 763 (2011)
3. D. Snoeck, K. Van Tittelboom, S.Steuperaert, P. Dubruel, N. De Belie, J. Intell. Mater. Syst. Struct. **25(1)**, 13 (2014)
4. ZX. Hu, XM. Hu, WM. Cheng, YY. Zhao, MY Wu, Constr. Build. **179**, 151 (2018)
5. Y. Shields, N. De Belie, A. Jefferson, K. Van Tittelboom, Smart Mater. Struct. **30** (2021)
6. Y. A. Villagrán Zaccardi, N. M. Alderete, N. De Belie, Cem. Concr. Res. **100**, 153 (2017)
7. K. J. Shin, W. Bae, SW. Choi, M.W. Son, K.M. Lee, Constr. Build. **151**, 907 (2017)
8. B. Van Belleghem, K. Van Tittelboom, N. De Belie, materconstrucc, **68**, 159 (2018)
9. C. Edvardsen, ACI Mater. J. **96**, 448 (1999)
10. T. Van Mullem, E. Gruyaert, B. Debbaut, R. Caspeele, N. De Belie, Constr. Build. **203**, 541 (2019)
11. D. Snoeck, S. Steuperaert, K. Van Tittelboom, P. Dubruel, N. De Belie, Cem. Concr. Res. **42**, 1113 (2012)
12. N. M. Alderete, Y. A. Villagrán Zaccardi, N. De Belie, Cem. Concr. Compos. **106** (2020)